Manuscript for: Separation and Purification Technology

Solubility of di-(2-ethylhexyl)phosphoric acid (D2EHPA) in aqueous electrolyte solutions: studies relevant to liquid-liquid extraction

Brent Grymonprez[†], Rayco Lommelen[†], Jakob Bussé[†], Koen Binnemans[†], Sofía Riaño[†]*

[†] KU Leuven, Department of Chemistry, Celestijnenlaan 200F, P.O. box 2404, B-3001 Leuven, Belgium.

B. Grymonprez, R. Lommelen, J. Bussé, K. Binnemans, S. Riaño
Separation and Purification Technology **333** (2024) 125846 (10 pages).
DOI: 10.1016/j.seppur.2023.125846

*Corresponding author:

Email: Sofia.Riano@kuleuven.be

Abstract

Di-(2-ethylhexyl)phosphoric acid (D2EHPA) is an acidic extractant frequently used in solvent extraction for metal refining. Only limited information is available on the amount and type of impurities present in commercially available D2EHPA and their effect on liquid-liquid extraction. In this paper, these impurities were identified and the importance of pre-conditioning the extractant before carrying out extractions is demonstrated. Furthermore, the solubility of D2EHPA in aqueous solutions was investigated as a function of pH, concentration of extractant and anion present in the aqueous phase (chloride, bromide, iodide, sulfate, methanesulfonate, thiocyanate, and nitrate). The density of the organic phases and the sodium and water uptake in the organic phase were determined as a function of the different anions present in the aqueous phase. The type of anion was found not to have a large influence on the solubility of D2EHPA in the aqueous phases. Low concentrations of salt in the aqueous phase or high pH values resulted in significant losses of D2EHPA to the aqueous phase. A very sharp increase in water content in the organic phase was observed around pH 5 (pH 6 for the nitrate system), accompanied by a significant increase in extraction of sodium ions, which explains the observed increase in density of the organic phase, and the tendency to third-phase formation. The results from this fundamental study help to better understand the behavior of liquid-liquid extraction systems in which D2EHPA is used as extractant and can help to prevent third-phase formation and losses of extractant to the aqueous phase. Moreover, the impurities present in commercially available D2EHPA and their impact on liquid-liquid extraction processes are determined.

Keywords: Acidic extractant; hydrometallurgy; liquid-liquid extraction; solubility; solvent extraction

1. Introduction

Solvent extraction (SX) or liquid-liquid extraction is one of the most often used techniques for the separation of metals in solution. Di-(2-ethylhexyl)phosphoric acid (D2EHPA) is one of the most popular acidic extractants due to its selectivity, versatility, commercial availability, good physicochemical properties, and chemical stability. For decades, D2EHPA has been employed in the separation of rare-earth elements [1–3], nickel and cobalt [4], indium and gallium [5], zinc [6], vanadium [7], and iron [8]. As an acidic extractant, D2EHPA extracts metal ions via the following (simplified) reaction mechanism:

$$\mathrm{M}_{(\mathrm{a})}^{\mathrm{n}+} + n\mathrm{HL}_{(\mathrm{o})} \rightleftarrows [\mathrm{ML}_n]_{(o)} + n\mathrm{H}_{(\mathrm{a})}^{+} \qquad [1]$$

With M^{n+} the aqueous metal ion, HL and L^- the undissociated and dissociated extractant, and (a) and (o) the aqueous and organic phases respectively. As it can be seen in Eq(1), the extraction and stripping can be controlled by varying the pH of the aqueous phase. Another characteristic of acidic extractants is that they tend to form dimers in non-polar diluents and at low metal loadings, whereas at high metal loadings and in polar diluents they can be found as a monomer [4,9]. It is also known that acidic extractants can form water-in-oil microemulsions or reverse micelles in the organic phase. In reverse micelles, the long alkyl chains of the extractant face outwards and are in contact with the diluent, while the charged head groups face inward encapsulating a rigid pool of water molecules. In water-in-oil microemulsions, the non-polar tails of the extractant point towards the organic phase while the polar heads are oriented

inwards, having mobile or free water molecules in the core that has an additional layer of rigidly-held water molecules that satisfies the hydration requirements of the head groups [10,11]. It has been demonstrated that saponification of D2EHPA leads to reverse micelle formation or water-in-oil microemulsions that affect the kinetics, the selectivity, and the degree of extraction [10,12–14]. Furthermore, these type of structures can agglomerate into wormlike or other geometries that can lead to third-phase formation during solvent extraction [10]. Until today a lot of efforts have been made to understand the behavior of the extractant in the organic phase, but little attention has been paid to the solubility of the extractant in the aqueous phase and the factors that influence it.

For the development of an economically feasible solvent extraction process, it is crucial that the extractant has low solubility in the aqueous phase and it is equally important to understand the factors that affect its solubility. In a liquid-liquid extraction process, this solubility depends mainly on three different factors: 1) the concentration of salts in the aqueous phase, because the salting-out effect effects helps to keep the organic extractant in the organic phase, 2) the pH of the aqueous solution, because high pH values deprotonate the extractant, transferring the extractant anion and its counter cation to the aqueous solution and make the organic phase prone to formation of reverse micelles and 3) the temperature, because usually the solubility of the organic components in the aqueous phase increases with increasing temperatures. There are only few studies concerning the solubility of D2EHPA in aqueous mixtures and some of the data are sometimes contradictory [15–17]. In some of these works, the sample of commercial D2EHPA was not treated to remove impurities prior to the solubility measurements[17,18]. These works were limited to either the study of the solubility in a 0.1 $mol \cdot L^{-1}$ chloride solution as a function of the pH and the D2EHPA concentration in the organic phase [15], in a 0.005 $mol \cdot L^{-1}$ H_2SO_4 solution as function of the composition of the organic phase, temperature and time [16], or in ammonium chloride, sulfate and nitrate

solutions as a function of the salt concentration, pH and loading of the organic phase[18]. Although the quantitative values found in these references might not be very accurate, some qualitative trends can be deduced from them: the solubility of D2EHPA in aqueous solutions increases with increasing the equilibrium pH above 2, the D2EHPA concentration in the organic phase or decreasing the salt concentration in the aqueous phase [15,18].

In this work, the sodium-D2EHPA-*n*-dodecane system is characterized as hardly any information about it is available and it is a common system studied in solvent extraction. The solubility of D2EHPA in the aqueous phase and the density, sodium content and water content of the organic phase were measured depending on the pH, the anion of the sodium salt, the salt concentration, the temperature and the D2EHPA concentration. The impurities present in commercially available D2EHPA have been detected and quantified, and their impact on liquid-liquid extraction processes is discussed. These studies can allow to estimate more accurately extractant losses due to solubility and to better understand the factors that influence the third-phase formation in liquid-liquid extraction.

2. Experimental

2.1. Chemicals

Di-(2-ethylhexyl)phosphoric acid (D2EHPA, 95 %), *n*-dodecane (99%, pure), ethylene glycol (99.5%), sodium bromide (99.5%, for analysis), sodium methanesulfonate (99%), were purchased from Acros Organics (Geel, Belgium). Sodium chloride (≥ 99.5%), sodium hydroxide (analytical grade, 99.25%), acetone (≥ 99.8%), sulfuric acid (≥ 95%), methyl-*tert*-butyl ether (≥ 99.5%), toluene (99.98%), ethanol, were purchased from Fisher Scientific (Merelbeke, Belgium). Nitric acid (65%), copper sulfate (anhydrous, 99%+), sodium sulfate (99%+), sodium nitrate (99.5%+), 0.1 mol·L^{-1} KOH, and ICP standard solutions of PO_4^{3-}, Ca, Na, In, Sr, and Sb were purchased from Chem-Lab (Zedelgem, Belgium). Hydrochloric acid (37%) was purchased from VWR chemicals (Haasrode, Belgium). Di-(2-ethylhexyl)phosphoric acid (97%), sodium iodide (≥ 99.5%, for analysis), deuterated chloroform (99.8% D, 0.1 v/v% TMS), potassium hydrogen phthalate, sodium tartrate dihydrate water standard for volumetric Karl Fisher titration and Triton X-100, were purchased from Merck (formerly Sigma-Aldrich, Darmstadt, Germany). Cesium chloride (≥ 99.9%) and sodium isothiocyanate (≥ 98%) were purchased from Carl Roth (Karlsruhe, Germany). Serva silicone solution in isopropanol for siliconizing quarts sample carriers was purchased from SERVA Electrophoresis (Heidelberg, Germany). MilliQ water was produced by a Reference A+ from Merck.

All chemicals were used as received, without any further purification, with the exception of D2EHPA. D2EHPA, either in its undiluted form or as 1 mol·L^{-1} solution in *n*-dodecane, was washed with 2 mol·L^{-1} HCl solution in an aqueous-to-organic volume ratio of 1:4 to remove inorganic phosphate impurities. The mixture was shaken in a separatory funnel for 2h with a Recipro Shaker RS-1 from Lab Companion set at a speed of 280 shakes per minute. The

mixture was allowed to settle for at least 1 hour until the phases were completely separated. Other purifying methods for D2EHPA were investigated, but have not been used further. Their description can be found in the electronic supporting information.

2.2. Instrumentation

The concentration of D2EHPA in aqueous solutions was measured using an Optima 8300 Inductively Coupled Plasma Optical Emission Spectrometer (ICP-OES, Perkin Elmer), with a Scott cross-flow nebulizer. The samples were made by taking an aliquot of the aqueous phase and diluting it with MilliQ water, aiming for a phosphate concentration between 0.5 and 10 ppm. If certain samples needed to be diluted more than others in a set, the MilliQ water was spiked to ensure an equal salt concentration across the whole set and therefore the same matrix effect. The calibration samples underwent the same treatment and consisted of solutions of 0; 0.2; 0.5; 1; 2; 5; and 10 ppm PO_4^{3-}. Phosphorus (P) can be directly measured with ICP-OES and there is no need to convert organophosphorus to orthophosphate. For the quantification of P (213.6 nm, radial mode), the standard curve equation corresponded to y= 84,81951x – 1,45048 with R^2=0,99987. Indium (50 ppm) was used as internal standard in the calibration curve and all the samples.

The sodium content of the organic phases was determined by stripping 2 mL of the samples with an equal volume of 3 mol·L^{-1} HCl. The samples were then diluted in MilliQ water for ICP-OES measurement, aiming at sodium concentrations between 1 and 20 ppm. The calibration samples consisted of 0; 0.1; 0.2; 0.5; 1; 2; 5; 10; 20 and 50 ppm Na. All samples, including the calibration samples, contained 600 ppm of cesium, which acted as ionization buffer. Without this buffer, different concentrations of easily ionized elements (such as sodium and the other alkali metals) could shift the ionization equilibrium, causing their spectral emissions to become more intense or less intense, depending on the conditions.

Adding a large amount (at least five times the amount of the analyte) of an easily ionized element such as cesium minimizes this interference [19]. Indium (50 ppm) was used as an internal standard to construct the calibration curve and in all the samples.

The water content of the samples was measured with either a C30s coulometric or a V30s volumetric Karl Fischer titrator of Mettler–Toledo, using a Stromboli oven to evaporate the water out of the samples at 150 °C and bubbling it through the titration solution via a dried nitrogen carrier gas stream. The samples were not added directly to the titrator because acids like D2EHPA can form esters by reaction with the methanol solvent of the Karl Fischer titration solution and release extra amount of water. The equilibrium pH was measured with a Mettler–Toledo S220 SevenCompact pH meter.

The density of the organic phase was determined with an Anton Paar DMA 4500 M density meter. About 1 mL of the sample was slowly introduced into the density chamber using a syringe. The internal camera allowed to verify that the chamber was completely filled without any air bubbles. When the chamber was completely and homogeneously filled with the sample, the measurement was started using the Anton Paar preset density method to determine the density at 25 °C.

^{1}H, ^{13}C and ^{31}P NMR spectra were recorded from the different samples of D2EHPA by diluting them in $CDCl_3$ containing TMS as internal standard. The samples were measured on a Bruker Advance III HD 400 MHz spectrometer, operating at 400 MHz for ^{1}H. The NMR spectra were analyzed by MestReNova software.

2.2.1. Autotitration measurements

An autotitrator (Mettler Toledo, Titrator Excellence T5) was used to measure the actual amount of D2EHPA and its mono-alkyl equivalent, mono-(2-ethylhexyl)phosphoric acid (M2EHPA) in the D2EHPA batch. Approximately 30 mg of D2EHPA was dissolved in

50 mL of high-purity acetone (> 99.8%) and 50 mL of MilliQ. The titrant, 0.1 $mol \cdot L^{-1}$ KOH, was standardized using a known amount of oven-dried potassium hydrogen phthalate. A potentiometer was used to measure the pH during the titration and the measurements were performed in triplicate. The first equivalence point at pH 5–6 marks the neutralization of all the protons of the D2EHPA molecules and the most acidic proton of M2EHPA. The second equivalence point at pH 8–9 marks the neutralization of the least acidic proton of M2EHPA. The quantity of M2EHPA can be calculated by subtracting the amount of acid neutralized for both equivalence points. Deducting the resulting M2EHPA quantity from the amount of acid neutralized at the first equivalence point allows to determine the amount of D2EHPA in the sample.

2.2.2. HPLC-MS measurements

High-performance liquid chromatography – mass spectrometry (HPLC-MS) measurements of the D2EHPA samples were recorded to determine all the impurities it contained. The HPLC unit consisted of a Prevail™ C18 column with a particle size of 3 µm, a length of 150 mm and an internal diameter of 2.1 mm. A solution of 0.1% formic acid in water was pumped for 40 min and then methanol for another 30 min. The flow rate was 0.12 $mL \cdot min^{-1}$, and the injection volume was 10 µL. The MS unit utilized electrospray ionization (ESI), and scanned positive ions in the range of 100 to 1500 m/z. The results were analyzed with the Spectrus Processor software from ACD/Labs to identify all the components.

2.2.3. TXRF measurements

To determine the extraction of halide ions to the organic phase, an S2 PICOFOX TXRF spectrometer (Bruker, Germany) was used, and the results were analyzed with the Bruker Spectra software. The quartz sample carriers were siliconized with SERVA and dried in an

oven at 60 °C for 20 min. Then, either a small drop of the pure organic phase, or a drop of a 10 vol% organic phase, 5 vol% aqueous internal standard (1000 ppm Ca for Cl, 1000 ppm Sr for Br, 1000 ppm Sb for I) and 85 vol% of a 20:80 vol% mixture of Triton X-100 in ethanol was placed on the carrier, and the sample carriers were then dried in an oven at 100 °C overnight before measurement.

2.3. Solubility and extraction experiments

All solubility and extraction experiments were performed in triplicate, except for those of varying the organic D2EHPA concentration and at higher temperatures. In the case where the experiments were performed in triplicate, their error bars (vertical for all, and also horizontal for values in function of the equilibrium pH) are drawn behind the data points of the figures and are not visible when they are smaller than their corresponding data points.

2.3.1. Solubility of D2EHPA in aqueous solutions

5 mL of aqueous solution was contacted with 5 mL of 1 $mol \cdot L^{-1}$ D2EHPA in *n*-dodecane in plastic centrifuge tubes (15 mL), unless otherwise stated. The aqueous phase consisted of MilliQ water, specific amounts of salt solution ranging from 0.1 to 1.8 $mol \cdot L^{-1}$ of sodium chloride, bromide, iodide, sulfate, methanesulfonate, nitrate or isothiocyanate, and either the acid corresponding to the salt used or sodium hydroxide.

For experiments in which the D2EHPA concentration was varied, 6 mL of each phase was used. The concentration of D2EHPA was varied between 0.1 $mol \cdot L^{-1}$ and 3.0 $mol \cdot L^{-1}$ (pure D2EHPA). The aqueous phase consisted of 0.1 $mol \cdot L^{-1}$ NaCl. The centrifuge tubes were shaken horizontally for two hours, at either room temperature in a MaxQ 2000 shaker from Thermo Scientific, or at 40 °C or 60 °C in a Thermoshake oven shaker from Gerhardt. After equilibration, the samples were centrifuged for at least 10 minutes at 4000 rpm in an Eppendorf 5804 centrifuge. Samples shaken at higher temperatures were left to settle in a

water bath of the same temperature overnight. The phases were then separated using Pasteur pipettes and the equilibrium pH was measured.

To measure the solubility of D2EHPA, 75 mL of 1.2 $mol \cdot L^{-1}$ of unwashed D2EHPA in *n*-dodecane was shaken with 75 mL 1.0 $mol \cdot L^{-1}$ Na_2SO_4 in a separatory funnel for 2h at room temperature. After separating the phases, the phosphorus content was measured with ICP-OES.

2.3.2. Sodium extraction

The samples consisted of 2 mL of 3 M HCl and 2 mL of the organic phases in 4 mL glass vials with plastic screwcaps. They were shaken in a MaxQ 2000 shaker from Thermo Scientific at room temperature for 1 hour, centrifuged for 10 min at 2000 rpm in a Labofuge 200 from Heraeus, and the aqueous phase transferred into new vials using Pasteur pipettes.

3. Results and discussion

3.1. Impurities in commercially available D2EHPA

Biswas et al. reported that the solubility of D2EHPA in aqueous solutions corresponded to 2.9 mg L^{-1} [15], whereas Azam et al., reported that it corresponded to 90 mg L^{-1} [17]. The former decomposed D2EHPA in the aqueous phase with sulfuric acid and used the molybdenum blue method for quantification of phosphorus while the latter used ICP-MS. In this work, the D2EHPA concentration in the aqueous phase was determined by quantifying phosphorus with ICP-OES. The results are summarized in Table 1.

Table 1: Solubility of D2EHPA in aqueous solutions at different conditions and measured with different analytical techniques.

Conditions	Analytical technique	[D2EHPA] ($mg \cdot L^{-1}$)	Reference
1.0 $mol \cdot L^{-1}$ Na_2SO_4 – 1.2 $mol \cdot L^{-1}$ D2EHPA in *n*-dodecane	ICP-OES	349	This work
	ICP-OES*	313	This work
	^{1}H NMR*	150 ± 15	This work
0.1 $mol \cdot L^{-1}$ total Cl (HCl + NaCl) – 0.2 $mol \cdot L^{-1}$ D2EHPA in *n*-dodecane	ICP-OES	193	This work
0.1 $mol \cdot L^{-1}$ NaCl – pure D2EHPA	ICP-OES	15	This work**
0.001 $mol \cdot L^{-1}$ H_2SO_4 – 0.2 mol·D2EHPA in Escaid 110	ICP-MS	~90	Azam 2010
0.1 $mol \cdot L^{-1}$ total Cl (HCl & NaCl) – 0.2 $mol \cdot L^{-1}$ D2EHPA in kerosene	Molybdenum blue	2.9	Biswas 2000

* Experiments performed in D_2O to verify if the results are similar to those in H_2O, for the ICP-OES the D_2O sample was diluted in non-deuterated aqueous media

**: After washing with 2 $mol \cdot L^{-1}$ NaCl

The discrepancies among the results could be explained by the presence of water-soluble phosphorus compounds in the commercially-available D2EHPA. Common impurities that have been mentioned in the literature are mono-(2-ethylhexyl)phosphoric acid (M2EHPA), tri-(2-ethylhexyl)phosphate (T2EHP), 2-ethylhexanol, other organics, iron ions, pyrophosphates and polyphosphates, with the latter two being most likely the discrepancy of the analytical results as they are the most water-soluble phosphorus compounds [20–23]. The structure of D2EHPA and some of its common impurities are given in Figure 1.

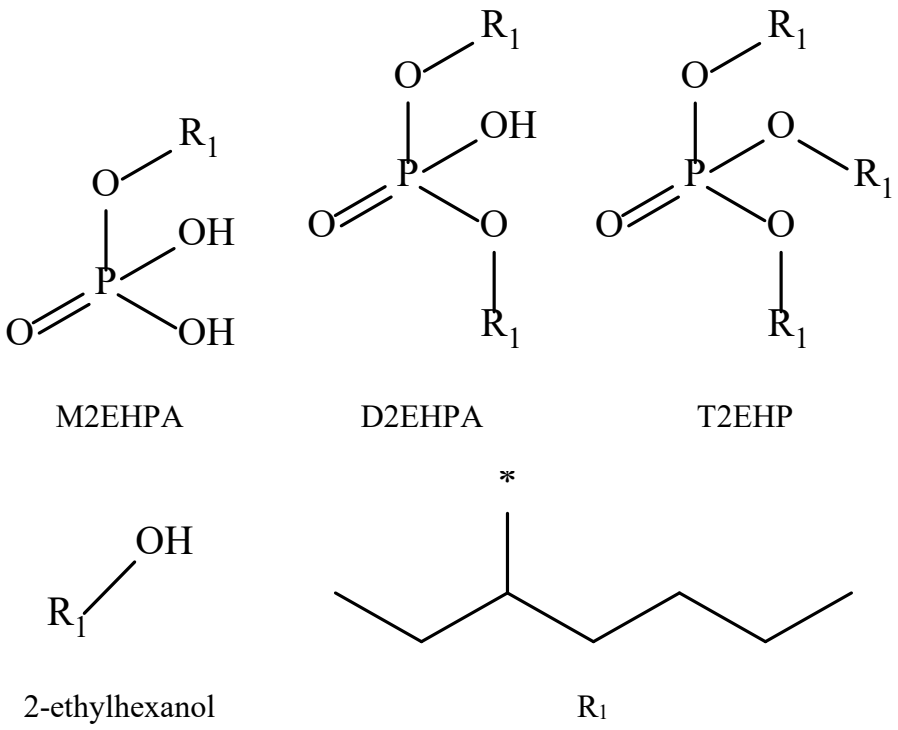

Figure 1. Structures of D2EHPA, M2EHPA, T2EHP and 2-ehtylhexanol. The carbon with an asterisk (*) of R_1 binds with the main structure.

To verify the hypothesis that the discrepancies among the results reported in Table 1 are due to the presence of other phosphorus-containing compounds, the organic phase containing D2EHPA was washed 10 times with fresh 2 $mol \cdot L^{-1}$ NaCl and the phosphorous content in the aqueous phase was determined with ICP-OES. Figure 2 shows that all the soluble impurities

are removed after a single wash, and the D2EHPA solubility in the aqueous phase corresponds to approximately 15 ppm.

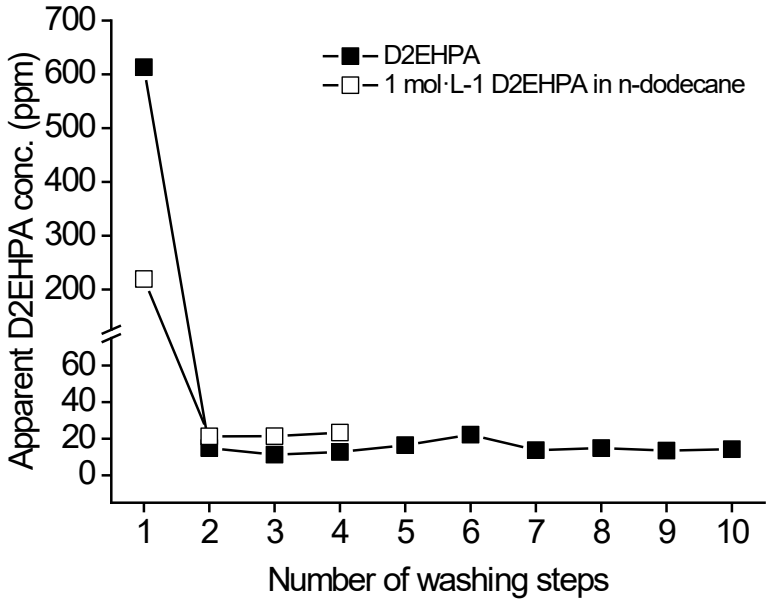

Figure 2: Measured apparent D2EHPA concentration in subsequent washing steps of the same organic phase with a fresh 2 mol·L^{-1} NaCl solution.

The differences between the concentrations reported in the different works can be explained. The molybdenum blue method most likely suffered from incomplete decomposition by the sulfuric acid and this led to an underestimation of the solubility of D2EHPA [15]. Apart from that, the method has been found to be less straightforward and some assumptions about it have been found to be wrong [24]. In the case of the work of Azam et al. where ICP-MS was used, a higher solubility of D2EHPA was reported [16,17]. This is probably because D2EHPA was not washed before the measurement and water-soluble impurities have led to an overestimation of the solubility.

The actual composition of the commercially available D2EHPA was studied. In the first approach, mass spectroscopy (MS) was used to identify all the constituents after separating them through high-performance liquid chromatography (HPLC). In the second approach, an autotitrator was used to determine the concentration of the pH-active constituents.

The HPLC-MS identified three species in the total ion current (TIC) chromatogram as seen in Figure S1 in the supporting information. The large peak at 50 min corresponds to D2EHPA =, mostly present in its protonated dimeric form [2(D2EHPA)+H^+]. The peak at 41 min is the more polar, and thus less retained, mono-(2-ethylhexyl)phosphoric acid (M2EHPA), the mono-alkyl equivalent of D2EHPA, in the form of the positively charged [M2EHPA+Na]$^+$, [2(M2EHPA)+H]$^+$ and [2(M2EHPA)+Na]$^+$ complexes. The last peak is from the more retained and less polar tri-(2-ethylhexyl)phosphate (T2EHP), in the form of [T2EHP+H]$^+$, [T2EHP+Na]$^+$, [2(T2EHP)+H]$^+$, and [2(T2EHP)+Na]$^+$. All identified complexes are listed in Table 2.

Table 2: Constituents identified in D2EHPA and their positively charged species measured by HPLC-MS.

Constituent	m/z	Species	Structure *
M2EHPA	233.3	$[MH_2+Na]^+$	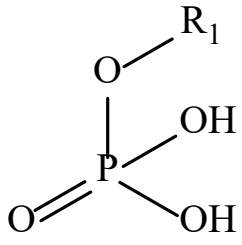
	421.4	$[2MH_2+H]^+$	
= MH_2 (MW = 210.21 $g \cdot mol^{-1}$)	443.3	$[2MH_2+Na]^+$	
	465.3	$[MH-MH_2+2Na]^+$	
D2EHPA	345.4	$[DH+Na]^+$	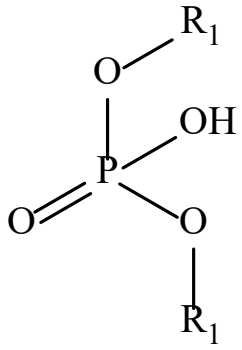
	645.6	$[2DH+H]^+$	
= DH (MW = 322.43 $g \cdot mol^{-1}$)	667.6	$[2DH+Na]^+$	
	689.5	$[D+DH+2Na]^+$	
	1011.7	$[D+2DH+2Na]^+$	
	1312.0	$[4DH+Na]^+$	
	1328.0	$[4DH+K]^+$	
T2EHP	435.5	$[T+H]^+$	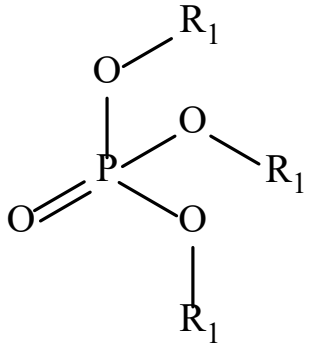
	457.5	$[T+Na]^+$	
= T (MW = 434.63 $g \cdot mol^{-1}$)	779.6	$[T+M+Na]^+$	
	869.8	$[2T+H]^+$	
	891.8	$[2T+Na]^+$	

* R_1 = 2-ethylhexyl-group

Neither ^{1}H, ^{13}C nor ^{31}P NMR of D2EHPA dissolved in deuterated chloroform could identify any other impurity, and the intensity of the proton peaks differs from the ideal values most likely due to the impurities.

The composition of D2EHPA was determined via titration with 0.1 mol·L^{-1} KOH using an autotitrator, as M2EHPA has two protons with different pK_a values and T2EHP does not contain any acidic protons. The difference between the protons originating from D2EHPA and the first protons from M2EHPA cannot be seen in the titration curve as their pK_a is very similar (1.42 for M2EHPA and 1.72 for D2EHPA)[25], and their inflection points coincide[26], so the composition cannot be calculated from this value alone. However, the protons neutralized between the equivalence point at pH 5 – 6 and the next at pH 7.5 – 9.5 all originate from the second dissociation step of M2EHPA. This number of protons allows to calculate the amount of M2EHPA, and by subtracting this number from the number of protons neutralized at the first equivalence point it is possible to obtain the amount of D2EHPA. By subtracting the mass of M2EHPA and D2EHPA from the original sample mass, the amount of T2EHP is calculated, assuming that any other impurity has a negligible presence. The composition was found to be 88.0 ± 0.4 w% D2EHPA, 3.97± 0.15 w% M2EHPA and 8.0 ± 0.2 w% T2EHP, which deviated substantially from the minimum purity of 95% mentioned on the label of the bottle. The titration curve can be found in Figure S2 in the Supporting Information. According to the manufacturer, the purity of the D2EHPA is checked by titration to pH 7 with 0.1 M NaOH, using phenolphthalein as an indicator, not taking into account the significant amount of M2EHPA present. With the molar mass of M2EHPA being around two-thirds that of D2EHPA, and M2EHPA releasing twice as many protons, the 4 w% of M2EHPA releases the same number of protons as if it were 12 wt% D2EHPA, coming to a false product purity of approximately 100%. Testing the purity of another bottle of D2EHPA labelled as 97% pure showed the presence of another impurity

being deprotonated at pH 9.5 – 10 which was found in the HPLC-MS spectra to have a molar mass of approximately 356 $g \cdot mol^{-1}$, although it could not be identified. The composition was found to be 87.5 ± 1.7 w% D2EHPA, 3.3 ± 0.7 w% M2EHPA and 9.2 ± 1.1 w% other compounds. It has been indicated in literature that 2-ethylhexanol could be another possible impurity [23], but it could not be identified in this work. The presence of certain impurities in D2EHPA (and in general in any extractant) can also lead to third-phase formation. Such impurities can extract other metal species that are prone to form crud and/or third phases. Furthermore, the presence of impurities with a relatively different polarity than the one of the extractant also promotes the formation of third-phases. Impurities with a different polarity may prevent the dissolution of the metal complex that is being extracted and/or may also entrain more water in the organic phase.

The description of the other studied methods to purify D2EHPA can be found in the Supporting Information. The D2EHPA used in this work was washed with 3 $mol \cdot L^{-1}$ HCl to remove the water-soluble phosphorus-containing impurities. Similar procedures using 0.5 $mol \cdot L^{-1}$ H_2SO_4 are also reported in the literature [27].

3.2. Influence of the concentration of D2EHPA in the organic phase on its aqueous solubility

When varying the concentration of D2EHPA in the organic phase, the solubility of D2EHPA in the aqueous phase reached a maximum value at 0.7 $mol \cdot L^{-1}$ total D2EHPA (Figure 3). As the equilibrium pH is higher than the pK_a of D2EHPA, most of the D2EHPA in the aqueous phase is present in its dissociated, negatively charged form. There seems to be no agreement in the literature on the pK_a of D2EHPA; the values range from 1.3 over 1.7 to even 2.75 [15,25,28,29]. It is known that measurement of the pKa of acids that are poorly water-soluble is an experimental challenge[30].

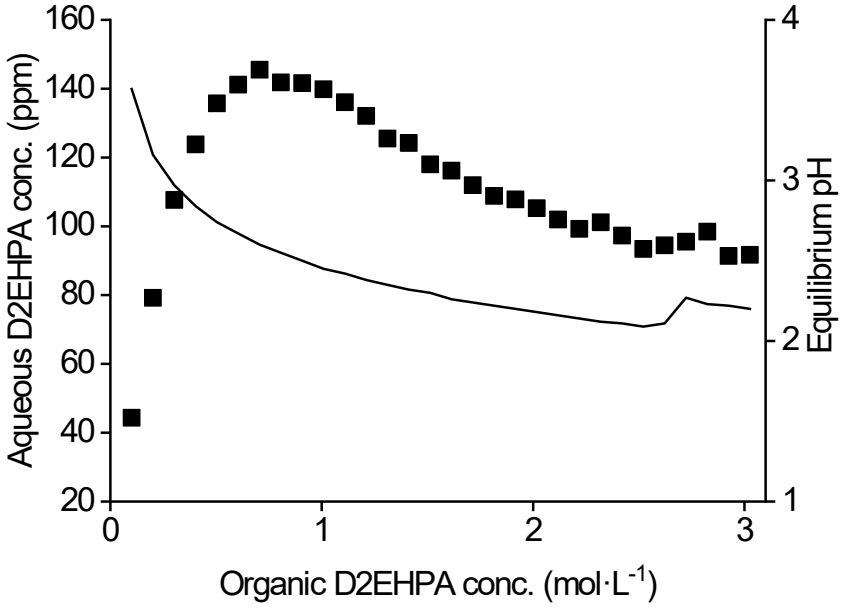

Figure 3: Concentration of D2EHPA in the aqueous phase as a function of the concentration of D2EHPA in the organic phase (markers) and the corresponding equilibrium pH values (line). Composition of the aqueous phase: 0.1 mol·L^{-1} NaCl, composition of the organic phase: from 0.1 mol·L^{-1} in *n*-dodecane to pure D2EHPA, contact time: 2 h.

Higher concentrations of D2EHPA in the organic phase increase the extraction of sodium by exchange with the D2EHPA proton (see Figure 4), which explains the decrease of the pH in the aqueous phase (Figure 3, line). The more acidic conditions caused by the increased sodium extraction are unfavorable for the D2EHPA to dissociate and this decreases its solubility in the aqueous phase.

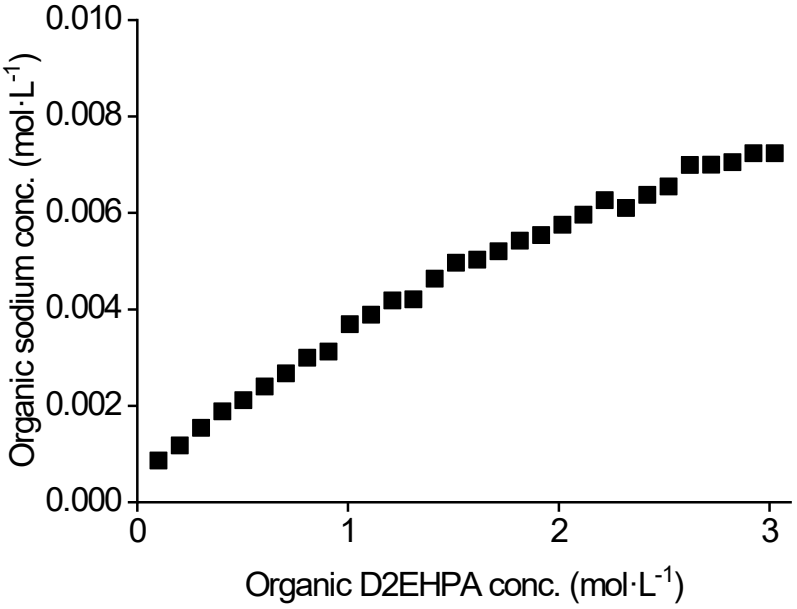

Figure 4: Concentration of sodium in the organic phase as a function of the concentration of D2EHPA (from 0.1 mol·L^{-1} D2EHPA in *n*-dodecane to pure D2EHPA). Contact time: 2h, 22 °C.. Composition of the aqueous phase: 0.1 mol·L^{-1} NaCl. Corresponding equilibrium pH values can be found on Figure 3.

3.3. Salting-out effect on the aqueous D2EHPA solubility

The solubility of D2EHPA in the aqueous phase mostly depends on the concentration of the salts present, and less on which salt is present. As it can be seen in Figure 5, the curves of the different salts lie closely together, and even intersect one another. Only the curve of sodium sulfate lies lower compared to the others due to the higher charge of the sulfate ions and the larger amount of sodium ions. At higher salt concentrations, the aqueous concentration of D2EHPA largely follows the Hofmeister series. The investigated ions are listed from largest salting-out effect to smallest in the following order: $SO_4^{2-} > CH_3SO_3^- > Cl^- > NO_3^- > Br^- > I^- > SCN^-$ [17,31]. The experimental values show that the nitrate ion has a slightly weaker salting-out effect than expected, being between the iodide and the isothiocyanate ions, and that the

effect of bromide and chloride ions is very similar. The larger error bars at the lower salt concentrations make it harder to compare the solubility values there.

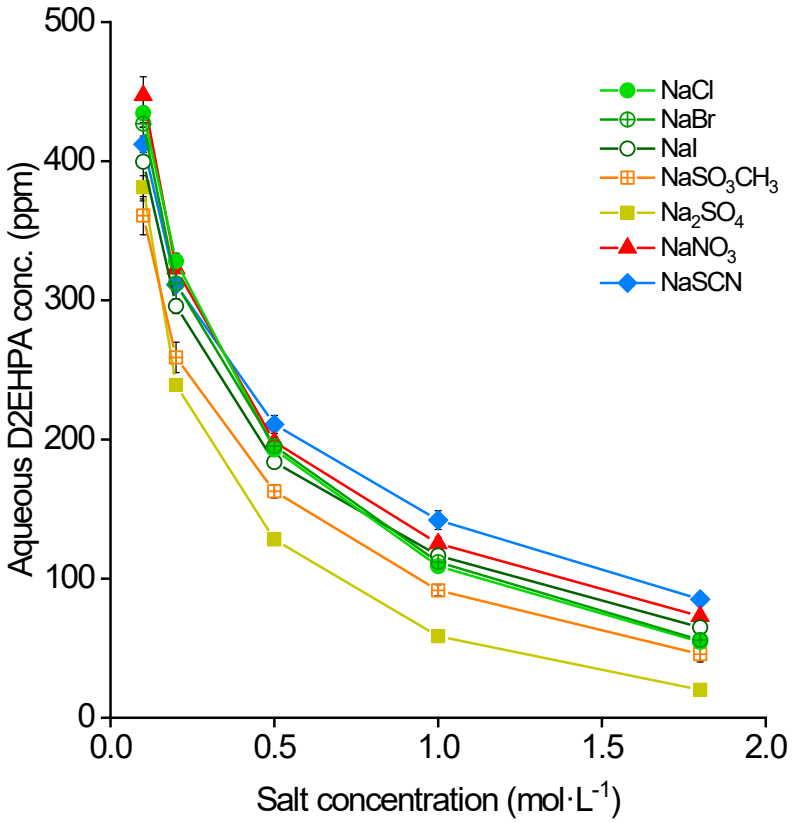

Figure 5: Solubility of D2EHPA (1 mol·L^{-1}) in different salt solutions (NaCl, NaBr, NaI, $NaSO_3CH_3$, Na_2SO_4, $NaNO_3$, NaSCN) with varying concentrations. Contact time: 2h, 22 °C.

The amount of sodium extracted to the organic phase is largely identical among the investigated ions and it increases at higher aqueous salt concentrations, except for the sulfate media, where a larger extraction is observed (Figure 6). This cannot be explained simply by the larger amount of sodium ions present in the aqueous phase, as plotting the graph in function of the starting sodium concentration instead of the anion concentration would still show a larger sodium uptake for the sulfate media compared to the other salts.

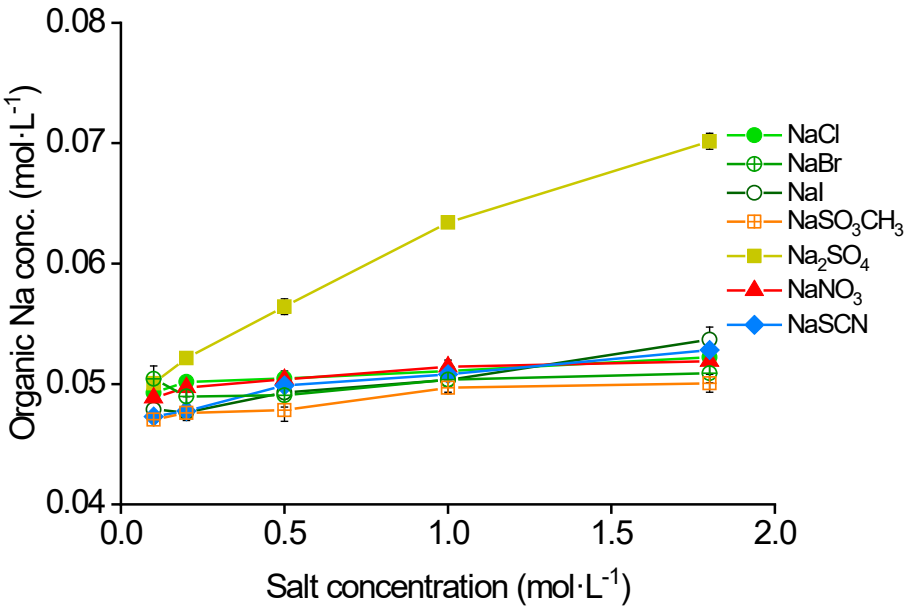

Figure 6: Extraction of sodium to the organic phase from the different salt solutions (NaCl, NaBr, NaI, $NaSO_3CH_3$, Na_2SO_4, $NaNO_3$, NaSCN) with varying salt concentrations. Contact time: 2h, 22 °C.

An additional effect might be the stronger salting-out effect of the sulfate ions, but as the other investigated ions hardly seem to affect the sodium extraction, this effect is most likely negligible. A third reason could be the pH buffering effect of the sulfate ions, which bind to the released acidic protons to form hydrogensulfate ions, which shifts the equilibrium towards the extraction. At the highest salt concentration, the pH of the aqueous sulfate phase is in the same range as that of the other salts (Table 3). Using the formula for the acid formation extent α_{HA} [32], see Equation 2, the extent of this proton removal can be calculated. The proton concentrations $[H^+]$ and the dissociation constant K_a can be converted to the pH and pK_a respectively, by using the latter as negative exponential factors of 10, see Equation 3.

$$\alpha_{HA} = \frac{[H^+]}{K_a + [H^+]} \quad [2]$$

$$\alpha_{HA} = \frac{10^{-pH}}{10^{-pK_a} + 10^{-pH}} \quad [3]$$

By taking HSO_4^- as the weak acid and its pK_a as 1.99,[33] and filling in the pH value of 2.63 at the highest sulfate concentration, the formula shows that 18.6% of the sulfate ions are protonated. Note that this formula does not take into account deviations from ideal, dilute solutions caused by the high ionic strength, so both the pK_a and the conversion of the pH to a proton concentration are merely crude estimates as they do not take the ion activities into account. To prevent this buffering effect from interfering, NaOH was added to reach a final concentration of 0.05 mol·L^{-1} in order to shift the equilibrium further towards extraction and a higher aqueous pH. Without it, all the curves were located approximately 1 pH unit lower, where comparison with the sulfate system was a lot harder. Adding more NaOH would cause trouble for obtaining a clear phase separation in the samples with the lowest salt concentrations.

Table 3: Equilibrium pH of the aqueous phases of the salting-out experiments.

	Salt concentration (mol·L^{-1})				
Salt	0.1	0.2	0.5	1.0	1.8
Na_2SO_4	3.57 ± 0.02	3.30 ± 0.02	2.99 ± 0.01	2.78 ± 0.01	2.63 ± 0.02
$NaSO_3CH_3$	4.06 ± 0.02	3.71 ± 0.02	3.29 ± 0.01	3.00 ± 0.01	2.73 ± 0.02

NaCl	3.94 ± 0.07	3.53 ± 0.02	3.08 ± 0.01	2.78 ± 0.02	2.46 ± 0.01
$NaNO_3$	3.86 ± 0.02	3.52 ± 0.01	3.12 ± 0.03	2.78 ± 0.01	2.52 ± 0.01
NaBr	3.99 ± 0.01	3.64 ± 0.02	3.16 ± 0.01	2.83 ± 0.00	2.51 ± 0.01
NaI	4.01 ± 0.10	3.78 ± 0.05	3.42 ± 0.02	3.12 ± 0.01	2.86 ± 0.01
NaSCN	3.96 ± 0.07	3.58 ± 0.02	3.13 ± 0.01	2.90 ± 0.11	2.66 ± 0.01

3.4. Effect of pH on the solubility of D2EHPA in aqueous solutions

The effect of the pH on the solubility of D2EHPA was investigated in chloride, sulfate and nitrate media, by adding different amounts of their respective acids or sodium hydroxide to the aqueous phases containing a final salt concentration of 0.3 $mol \cdot L^{-1}$. In Figure 7 it can be seen how the solubility of D2EHPA increases as the equilibrium pH increases. At equilibrium pH values higher than 5, larger standard deviations for both the D2EHPA concentration in the aqueous phase as in pH values are seen. At this point, whereas the sulfate system reaches a plateau, the chloride and nitrate systems show a further increase in aqueous D2EHPA solubility. The salting-out effects between the three anions also become very clear, much more than in the salting-out experiments, with differences larger than 100 ppm. All systems presented good phase disengagement until pH values around 6 – 6.5. Above this pH, a gel was formed in the organic phase.

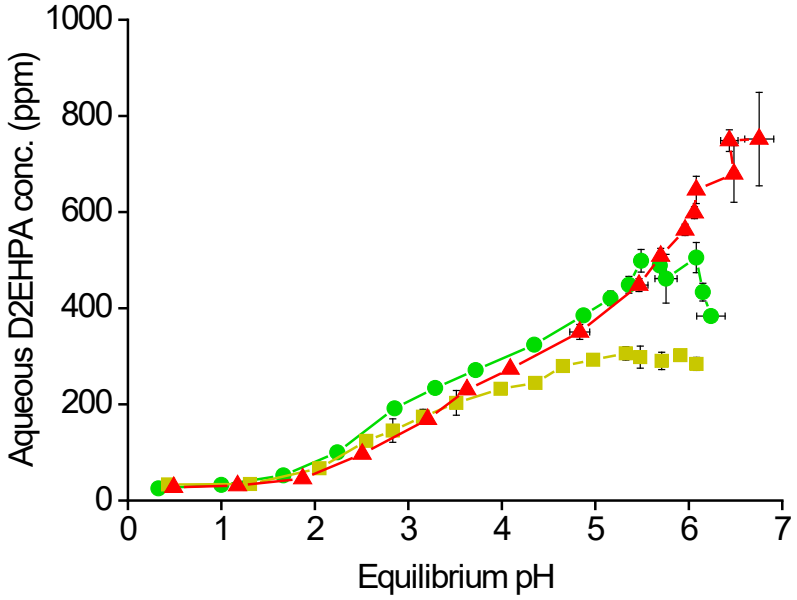

Figure 7: D2EHPA solubility in 0.3 mol·L^{-1} chloride (green circles), sulfate (yellow squares) and nitrate (red triangles) media as a function of the equilibrium pH. Contact time: 2h, 22 °C.

At the highest pH values, third and even fourth phases were formed. It was found that the top phase did not contain sodium and its density (23 °C) corresponded to the one of pure *n*-dodecane. At high equilibrium pH values, D2EHPA gets deprotonated by extracting sodium and forms third-phases or gels. The much rarer fourth phase was formed at the very bottom of the samples, but could not be investigated due to its small volume.

The sodium uptake shows a steady increase with rising pH, and only a small difference between the different media, as seen in Figure 8. The salting-out effect of the anions most likely causes this small difference. As the sulfate ion has a stronger salting-out effect and lowers the D2EHPA solubility with water, it also increases the removal of sodium from the aqueous phase by extraction, resulting in a larger concentration of sodium in the organic phase.

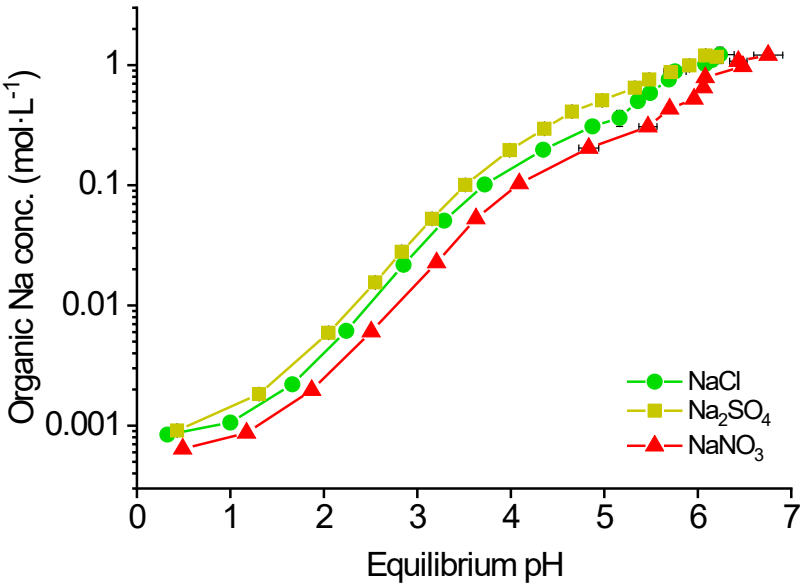

Figure 8: Concentration of sodium in the organic phase as a function of the aqueous equilibrium pH of the three salt systems (0.3 mol·L^{-1}) : chloride (green circles), sulfate (yellow squares) and nitrate (red triangles). Contact time: 2h, 22 °C.

3.5. Temperature effect on the solubility of D2EHPA in the aqueous phase

No temperature-dependence was observed for the solubility of D2EHPA or the extraction of sodium between 22 and 60 °C. The results can be found in the Electronic Support Information in Figures S3-S6.

3.6. Density of the organic phase

The density of the organic phase was measured as a function of the concentration of D2EHPA. Figure 9 shows that the density increases linearly when increasing the concentration of D2EHPA in the organic phase.

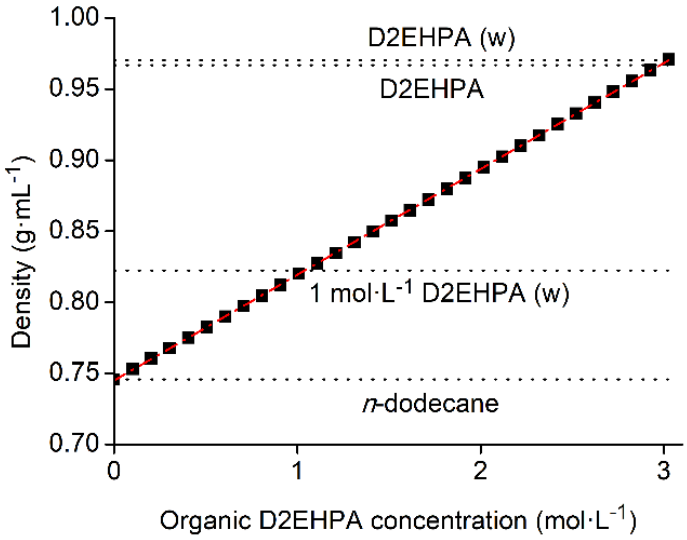

Figure 9: Density (measured at 22 °C) of the organic phase when varying its D2EHPA concentration. The horizontal dotted lines are, from bottom to top, the density of *n*-dodecane at 0.74586 g·mL^{-3}; 1 mol·L^{-1} D2EHPA in *n*-dodecane washed with 2 mol·L^{-1} HCl at 0.82239 g·mL^{-3}; D2EHPA at 0.96676 g·mL^{-3}; and D2EHPA washed with 2 mol·L^{-1} HCl at 0.97021 g·mL^{-3}. A dotted trend line is calculated through the points, with a formula of y = 0.74499 + 0.07443·x and an R^2-value of 0.99997.

The density as a function of the salt present in the aqueous phase was also studied (Figure 10). There is a small difference between the densities of the organic phases after contacting them with aqueous phases that contain different anions. The higher density of the organic phases that were contacted with aqueous solutions containing bromide and iodide was initially thought to be due to the co-extraction of those anions to the organic phase, but their presence was not detected by TXRF. For the organic phases contacted with sodium sulfate, a small

increase in density is observed when increasing the salt concentration. This can be attributed to the increased sodium extraction in those samples.

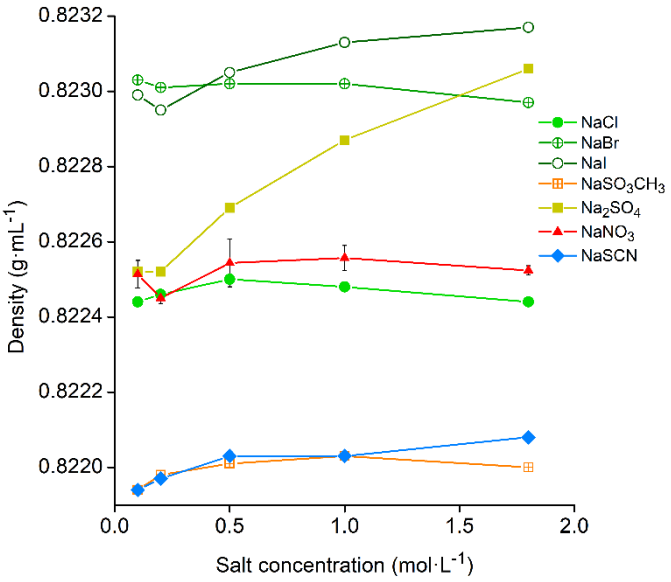

Figure 10: Density (measured at 22 °C) of the organic phases as a function of the salt and salt concentration of the aqueous phase they were in contact with. Note the very small range on the Y-axis. Only the nitrate samples were measured in triplicate.

Next, the effect of the equilibrium pH on the density was studied. As seen in Figure 11, the density of the organic phase starts increasing around pH 4, before rising sharply around pH 6. This is due to the water uptake in the organic phase. The sulfate system starts rising at lower pH values compared to the nitrate system, likely due to the higher Na update in the sulfate system.

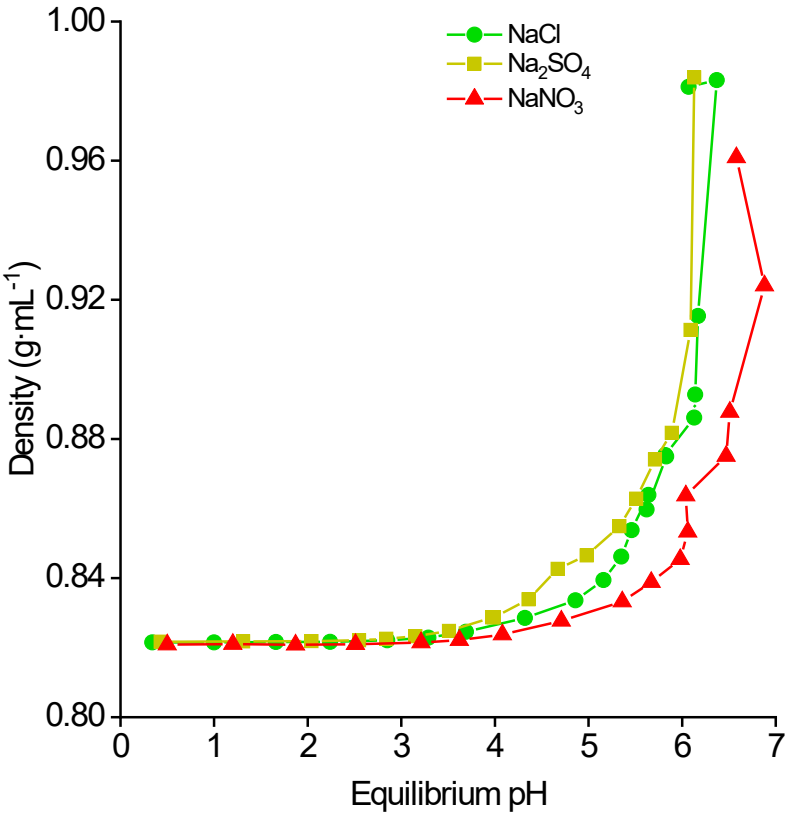

Figure 11: Density (measured at 22 °C) of the organic phase depending on the aqueous equilibrium pH value for the chloride (green circles), sulfate (yellow squares) and nitrate (red triangles) system. Salt concentration corresponds to 0.3 mol·L^{-1}.

Finally, the temperature effect on the density was measured. Figure 12 shows that increasing the temperature from 22 °C to 40 °C at a lower pH value decreases the density by approximately 0.01 g·cm^{-3}, and a further increase to 60 °C leads to a further decrease in density of approximately 0.01 g·cm^{-3}. At higher pH values, this difference in density changes is most likely due to a different water content.

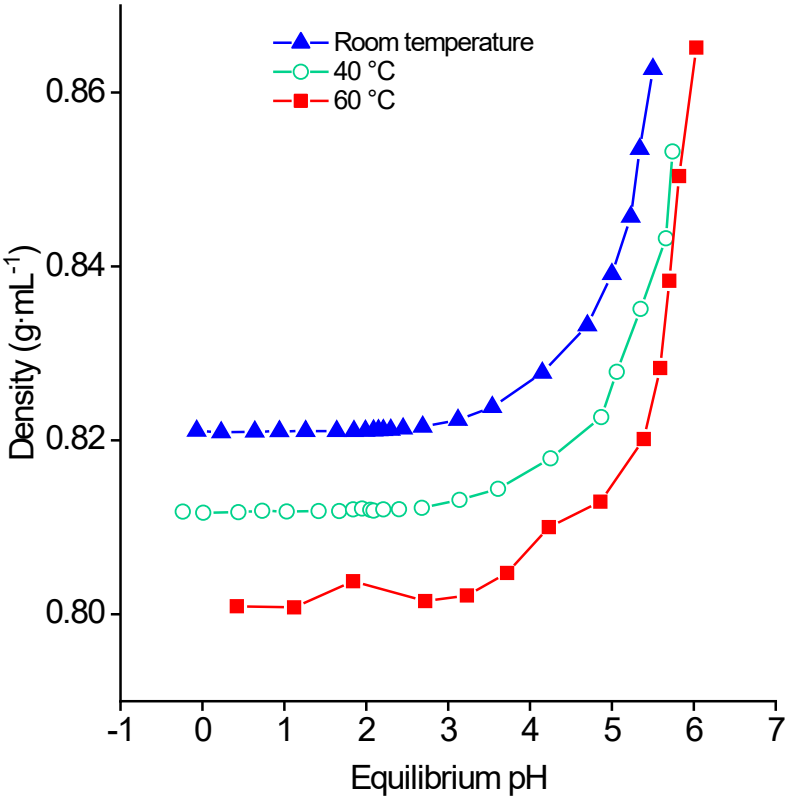

Figure 12: Density of the organic phase as a function of the aqueous equilibrium pH after contact with a 0.5 mol·L^{-1} $NaNO_3$ solution for 22 and 40 °C and 0.3 mol·L^{-1} $NaNO_3$ for 60 °C.

3.7. *Water uptake into the organic phase*

Finally, the water content of the organic phases was determined. When varying the concentration of D2EHPA in the organic phase, there is a steady increase with increasing D2EHPA concentration (Figure 13). The percentage of water in the organic phase increases almost linearly with the concentration of D2EHPA, as does the density (Figure 9). This shows that D2EHPA and *n*-dodecane behave like ideal liquids.

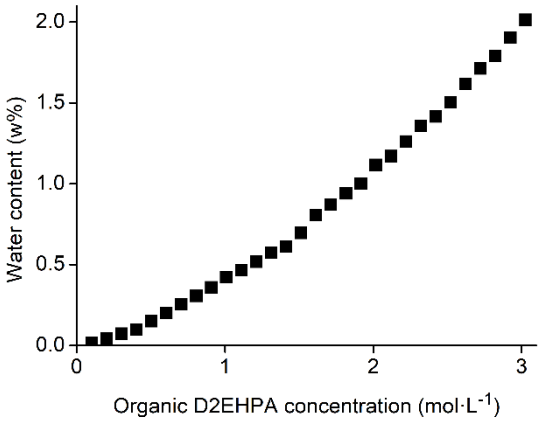

Figure 13: Water content of the organic phase as a function of the D2EHPA concentration.

The effect of different salts in the aqueous phase on the water content in the organic phase was determined. As can be seen in Figure 14, only the methanesulfonate system, and to a lesser extent the nitrate system, show a higher water content at the low concentrations of salt in the aqueous phase. All the other systems show similar and constant amounts of water in the organic phase. As mentioned before, no correlation was found between the water content and the density of the organic phases, as the methanesulfonate system has the lowest density, yet the highest water content.

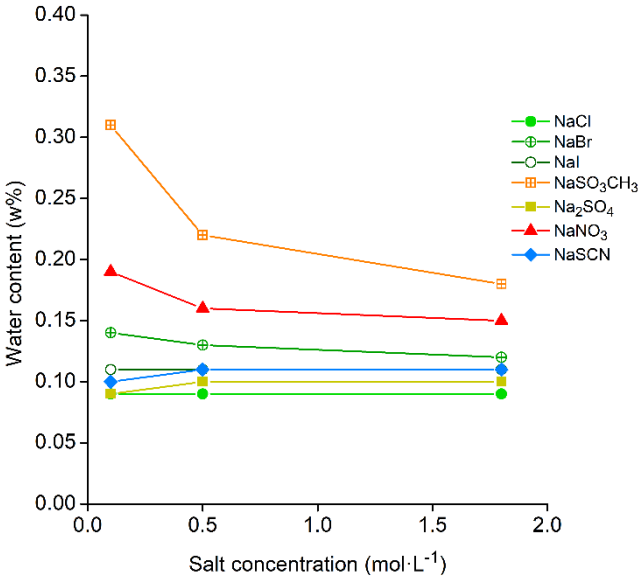

Figure 14: Water content of the organic phase as a function of the different aqueous salts and salt concentrations.

Finally, the water content of the organic phase was measured in function of the equilibrium pH. This showed a steep increase for the sulfate and chloride systems starting from pH 4 and for the nitrate from pH 5, as can be seen in Figure 15. This is most likely due to the different salting-out strength, where the uptake of water follows the extraction of sodium. The reason for this increased water content is most likely the formation of inverse micelles in the organic phase. Inverse micelles are aggregates of surfactants, in which their polar head groups form the inside surface of a sphere or tube, while their alkyl chains are in contact with the organic solvent. Inside these spheres or tubes, water is present in a bound and trapped state, and when the amount of water increases, the inverse micelles grow in size and the water behaves more as if it were free [34]. When the pH is higher and more sodium is extracted to the organic phase, there is a larger amount of Na-D2EHP complexes that can form these inverse micelles.

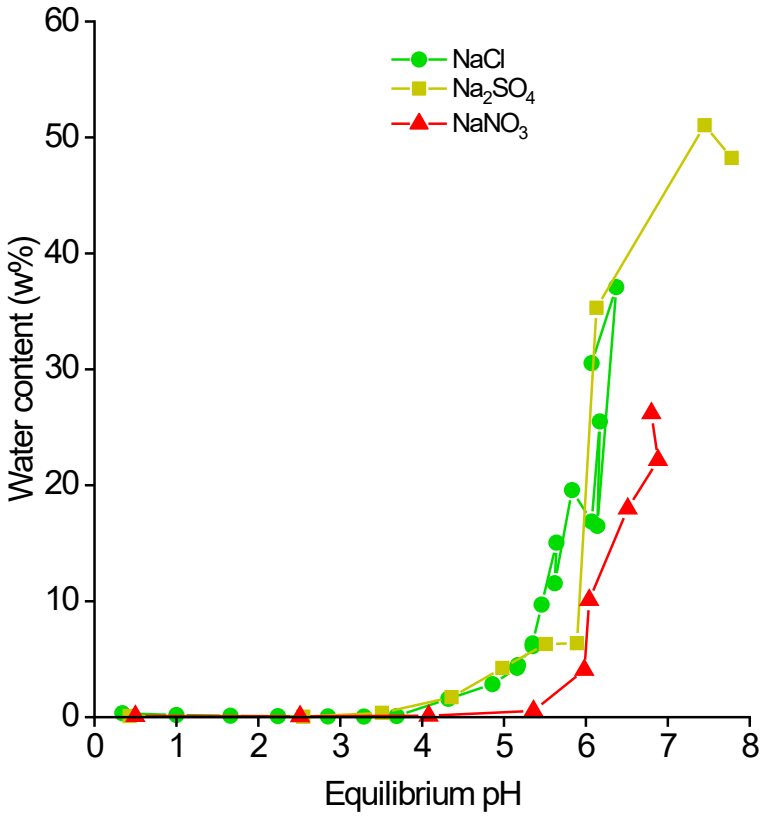

Figure 15: Water content of the organic phase as a function of the aqueous equilibrium pH of the chloride (green circles), sulfate (yellow squares) and nitrate (red triangles) systems.

4. Conclusions

The solubility of D2EHPA in the aqueous phase was found to depend primarily on the equilibrium pH of the aqueous phase and the salt concentration, and to a lesser extent on the anion of the salt present in the aqueous solution. The organic D2EHPA concentration has an influence as well. pH values above 5 should be avoided in extraction experiments due to the increased water uptake and tendency to third-phase formation. The sodium uptake and organic density are largely dependent on the aqueous pH, and only to a lesser extent on which salt was present in the aqueous phase. The temperature did not have a significant effect on the solubility of D2EHPA in the aqueous phase. The composition of D2EHPA was found to be 88.0 ± 0.4 w% D2EHPA, 3.97± 0.15 w% M2EHPA and 8.0 ± 0.2 w% T2EHP, which deviated substantially from the minimum purity of 95% mentioned on the label of the commercially available product. It is strongly recommended to wash a fresh batch of D2EHPA with water to remove impurities that are soluble in water before solvent extraction experiments.

Supporting Information

The Supporting Information contains the following:

- Chromatogram of D2EHPA
- Other D2EHPA purification methods
- Titration curve of D2EHPA containing M2EHPA impurity
- Effect of temperature on the solubility of D2EHPA in the aqueous phase and on the extraction of sodium ions

Acknowledgements

The authors would like to thank Bart Van Huffel for the HPLC-MS measurements. The research was funded by the European Research Council (ERC) under the European Union's Horizon 2020 Research and Innovation Programme: Grant Agreement 694078—Solvometallurgy for Critical Metals (SOLCRIMET).

Conflict of interest

There are no conflicts to declare.

References

[1] D.F. Peppard, G.W. Mason, J.L. Maier, W.J. Driscoll, Fractional extraction of the lanthanides as their di-alkyl orthophosphates, J. Inorg. Nucl. Chem. 4 (1957) 334–343. https://doi.org/10.1016/0022-1902(57)80016-5.

[2] K.A. Rabie, A group separation and purification of Sm, Eu and Gd from Egyptian beach monazite mineral using solvent extraction, Hydrometallurgy. 85 (2007) 81–86. https://doi.org/10.1016/j.hydromet.2005.12.012.

[3] W. Wang, Y. Pranolo, C.Y. Cheng, Recovery of scandium from synthetic red mud leach solutions by solvent extraction with D2EHPA, Sep. Purif. Technol. 108 (2013) 96–102. https://doi.org/10.1016/J.SEPPUR.2013.02.001.

[4] K. Sarangi, B.R. Reddy, R.P. Das, Extraction studies of cobalt (II) and nickel (II) from chloride solutions using Na-Cyanex 272.: Separation of Co(II)/Ni(II) by the sodium salts of D2EHPA, PC88A and Cyanex 272 and their mixtures, Hydrometallurgy. 52 (1999) 253–265. https://doi.org/10.1016/S0304-386X(99)00025-0.

[5] M.S. Lee, J.G. Ahn, E.C. Lee, Solvent extraction separation of indium and gallium from sulphate solutions using D2EHPA, Hydrometallurgy. 63 (2002) 269–276. https://doi.org/10.1016/S0304-386X(02)00004-X.

[6] D.D. Pereira, S.D.F. Rocha, M.B. Mansur, Recovery of zinc sulphate from industrial effluents by liquid–liquid extraction using D2EHPA (di-2-ethylhexyl phosphoric acid), Sep. Purif. Technol. 53 (2007) 89–96. https://doi.org/10.1016/J.SEPPUR.2006.06.013.

[7] G. Hu, D. Chen, L. Wang, J. Liu, H. Zhao, Y. Liu, T. Qi, C. Zhang, P. Yu, Extraction of vanadium from chloride solution with high concentration of iron by solvent

extraction using D2EHPA, Sep. Purif. Technol. 125 (2014) 59–65. https://doi.org/10.1016/J.SEPPUR.2014.01.031.

[8] R.K. Biswas, D.A. Begum, Solvent extraction of Fe^{3+} from chloride solution by D2EHPA in kerosene, Hydrometallurgy. 50 (1998) 153–168. https://doi.org/10.1016/S0304-386X(98)00048-6.

[9] A.M. Wilson, P.J. Bailey, P.A. Tasker, J.R. Turkington, R.A. Grant, J.B. Love, Solvent extraction: the coordination chemistry behind extractive metallurgy, Chem. Soc. Rev. 43 (2014) 123–134. https://doi.org/10.1039/c3cs60275c.

[10] S. Gao, T. Sun, Q. Chen, X. Shen, Characterization of reversed micelles formed in solvent extraction of thorium(IV) by bis(2-ethylhexyl) phosphoric acid. Transforming from rodlike to wormlike morphology, Radiochim. Acta. 104 (2016) 457–469. https://doi.org/10.1515/ract-2015-2538.

[11] S.P. Moulik, B.K. Paul, Structure, dynamics and transport properties of microemulsions, Adv. Colloid Interface Sci. 78 (1998) 99–195. https://doi.org/10.1016/S0001-8686(98)00063-3.

[12] J. Wu, H. Gao, D. Chen, T. Jin, S. Li, Microemulsion formation in some extractants and its effects on extraction mechanism, Sci. Sin. (Engl. Ed.); 23:12 (1980).

[13] N.M. Murashova, S.Y. Levchishin, E. V. Yurtov, Effect of Bis-(2-ethylhexyl)Phosphoric Acid on Sodium Bis-(2-ethylhexyl)Phosphate Microemulsion for Selective Extraction of Non-Ferrous Metals, J. Surfactants Deterg. 17 (2014) 1249–1258. https://doi.org/10.1007/S11743-014-1598-X.

[14] Y. Liu, M. Lee, G. Senanayake, Potential connections between the interaction and extraction performance of mixed extractant systems: A short review, J. Mol. Liq. 268

(2018) 667–676. https://doi.org/10.1016/J.MOLLIQ.2018.07.097.

[15] R.K. Biswas, M.A. Habib, M.N. Islam, Some physicochemical properties of (D2EHPA). 1. Distribution, dimerization, and acid dissociation constants of D2EHPA in a kerosene/0.10 kmol m-3 $(Na^+,H^+)Cl^-$ system and the extraction of Mn(II), Ind. Eng. Chem. Res. 39 (2000) 155–160. https://doi.org/10.1021/ie9902535.

[16] M.A. Azam, S. Alam, F. Khan, The Solubility/Degradation Study of Organophosphoric Acid Extractants in Sulphuric Acid Media, J. Chem. Eng. 25 (2010) 18–21. https://doi.org/10.3329/jce.v25i0.7235.

[17] M.A. Azam, Investigation of organic losses in solvent extraction circuit due to solubility/degradation, PhD thesis, Memorial University of Newfoundland, 2010.

[18] W. Su, J. Chen, Y. Jing, Aqueous Partition Mechanism of Organophosphorus Extractants in Rare Earths Extraction, Ind. Eng. Chem. Res. 55 (2016) 8424–8431. https://doi.org/10.1021/acs.iecr.6b01709.

[19] Y. Morishige, A. Kimura, Ionization interference in inductively coupled plasma-optical emission spectroscopy, SEI Tech. Rev. (2008) 106–111.

[20] W.J. McDowell, P.T. Perdue, G.N. Case, Purification of di(2-ethylhexylp)phosphoric acid, J. Inorg. Nucl. Chem. 38 (1976) 2172–2129. https://doi.org/10.1016/0022-1902(76)80486-1.

[21] J.A. Partridge, R.C. Jensen, Purification of di-(2-ethylhexyl)phosphoric acid by precipitation of copper(II)di-(2-ethylhexyl)phosphate, J. Inorg. Nucl. Chem. 31 (1969) 2587–2589. https://doi.org/10.1016/0022-1902(69)80591-9.

[22] J.M. Schmitt, C.A.J. Blake, Purification of di(2-ethylhexyl)-phosphoric acid, Oak Ridge National Lab, Tennessee, 1964.

[23] V. Hancil, M.J. Slater, W. Yu, On the possible use of di-(2-ethylhexyl) phosphoric acid/zinc as a recommended system for liquid-liquid extraction: the effect of impurities on kinetics, Hydrometallurgy. 25 (1990) 375–386. https://doi.org/10.1016/0304-386X(90)90052-4.

[24] E.A. Nagul, I.D. McKelvie, P. Worsfold, S.D. Kolev, The molybdenum blue reaction for the determination of orthophosphate revisited: Opening the black box, Anal. Chim. Acta. 890 (2015) 60–82. https://doi.org/10.1016/j.aca.2015.07.030.

[25] S. Acharya, A. Nayak, Separation of D2EHPA and M2EHPA, Hydrometallurgy. 19 (1988) 309–320.

[26] Y. Ramachandra Rao, S. Acharya, A rapid titrimetric determination of D2EHPA and M2EHPA, Hydrometallurgy. 32 (1993) 129–135. https://doi.org/10.1016/0304-386X(93)90062-I.

[27] F. Principe, G.P. Demopoulos, The solubility and stability of organophosphoric acid extractants in H_2SO_4 and HCl media, Hydrometallurgy. 68 (2003) 115–124. https://doi.org/10.1016/S0304-386X(02)00206-2.

[28] P. Kazemi, M. Peydayesh, A. Bandegi, T. Mohammadi, O. Bakhtiari, Pertraction of methylene blue using a mixture of D2EHPA/M2EHPA and sesame oil as a liquid membrane, Chem. Pap. 67 (2013) 722–729. https://doi.org/10.2478/s11696-013-0374-0.

[29] K. Omelchuk, P. Szczepański, A. Shrotre, M. Haddad, A. Chagnes, Effects of structural changes of new organophosphorus cationic exchangers on a solvent extraction of cobalt, nickel and manganese from acidic chloride media, RSC Adv. 7 (2017) 5660–5668. https://doi.org/10.1039/C6RA21695A.

[30] B.A. Wellen, E.A. Lach, H.C. Allen, Surface pKa of octanoic, nonanoic, and decanoic fatty acids at the air–water interface: applications to atmospheric aerosol chemistry, Phys. Chem. Chem. Phys. 19 (2017) 26551–26558. https://doi.org/10.1039/C7CP04527A.

[31] X. Gao, Hofmeister series at the liquid/liquid interface, PhD thesis, State University of New Jersey, 2016.

[32] J.-L. Burgot, Ionic Equilibria in Analytical Chemistry, Springer New York, New York, 2012. https://doi.org/10.1007/978-1-4419-8382-4.

[33] D.D. Perrin, Ionisation Constants of Inorganic Acids and Bases in Aqueous Solution, Elsevier, 1982. https://doi.org/10.1016/C2013-0-13276-X.

[34] T.H. Ibrahim, An Overview of the Physiochemical Nature of Metal-Extractant Species in Organic Solvent/Acidic Organophosphorus Extraction Systems, Sep. Sci. Technol. 46 (2011) 2157–2166. https://doi.org/10.1080/01496395.2011.594478.